

Behaviors of lead rubber bearing under horizontal bi-directional loading test

Takahito Nakamura & Osamu Kouchiyama

OILES Corporation, Tochigi, Japan

M. Kikuchi

Hokkaido University, Hokkaido, Japan



SUMMARY

Bi-directional horizontal loads were applied to lead rubber bearings (LRBs) to investigate the varying characteristics and torsional deformation of LRBs with different cross sections. Three types of specimens were used that had identical design characteristic values and a varying cross section: single-lead-plug circular and square LRBs, and a quadruple-lead-plug square LRB. As a result of the testing, it was found that the single-lead-plug circular and square LRBs exhibited identical characteristics and torsional deformation under bi-directional loading. It was, however, revealed that the quadruple-lead-plug square LRB suffered smaller torsional deformation than the other specimens. Its characteristic value was slightly different from that of the other specimens.

Keywords: bi-directional loading, input of phase difference, torsional moment, torsional deformation, square LRB, lead plug arrangement

1. INTRODUCTION

Seismically isolated buildings in Japan are composed of lead rubber bearings (LRBs), high damping rubber (HDR) bearings or natural rubber bearings (RBs) with no damping properties combined with dampers. Seismically isolated buildings were found to be effective as seismic resistant structures during the Great East Japan Earthquake that occurred on March 11, 2011. This is attributable to the development of conventional design methods and to the accumulation of test and evaluation data on isolators.

With the completion of large test apparatuses, it became possible to test and evaluate isolators using full-scale specimens. Bi-directional horizontal loading tests have recently been conducted for large specimens using multiple degree of freedom test apparatuses such as the SRMD (seismic response modification device) at the University of California, San Diego [1]. Minewaki et al. conducted bi-directional horizontal loading tests for HDR bearings using SRMD and verified such phenomena as the torsional deformation of HDR with damping properties, variation of hysteretic damping characteristics and deterioration of the critical strain capacity. LRBs have been reported to be subjected to neither extreme torsional deformation nor variations of hysteretic characteristics [2]. The authors conducted bi-directional horizontal loading tests for a full-scale 900 mm x 900 mm square LRB with four lead plugs symmetrically arranged in the cross section, and confirmed the soundness of LRB [3]. Few bi-directional horizontal loading tests have, however, been carried out for LRBs. No adequate data is available for investigating the occurrence of torsional deformation and the variations of hysteretic characteristics due to loading. LRBs in particular offer a high degree of freedom of design. In addition to laminating rubber, the rubber cross section may be either circular or square, and the number and arrangement of lead plugs can be selected and the cross sectional area of the lead plug

can be determined freely. Identifying the characteristics of LRB under bi-directional horizontal loading therefore requires testing and evaluation using the design elements of LRB as parameters.

In this study, bi-directional horizontal loading tests were conducted focused on the cross section of LRB (circular or square) and on the arrangement of lead plugs to investigate the characteristics under loading

2. TEST PLAN

2.1. Specimens

Three types of specimens were developed (Figure 1): a 225-mm-diameter single-lead-plug circular LRB (R1), single-lead-plug 200 mm x 200 mm square LRB (S1) and a quadruple-lead-plug 200 mm x 200 mm square LRB (S2). The specifications for the specimens are listed in Table 1. In the R1 circular LRB and S1 square LRB, a 40-mm-diameter lead plug was positioned at the center of the cross section. In the S2 square LRB, four 20-mm-diameter lead plugs were arranged symmetrically at the center. These specimens had the same sectional areas of rubber and lead, and the same total thickness of rubber layer. They had the same design characteristic value. Comparing the characteristics of R1 and S1 under loading was expected to enable the verification of difference attributable to the cross section of laminated rubber. Comparing S1 and S2 was expected to verify the difference due to lead plug arrangement. Three specimens of each type were made to be subjected to different loading conditions that are described below.

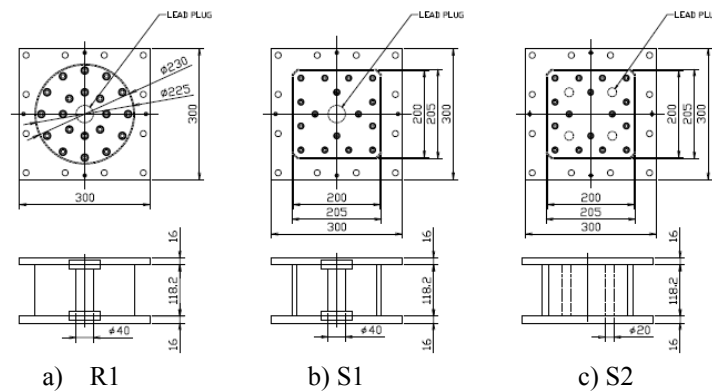


Figure1. Specimens

Table1. Specifications for the specimens

Specimen	LRB ϕ 225Pbx1	LRB \square 200Pbx1	LRB \square 200Pbx4
Code name	R1	S1	S2
Shape	Circular	Square	←
Rubber layer mm	225	200	←
Lead plug diameter mm	40	40	20
Led plug number mm	1	1	4
Rubber section area mm ²	38504	38543	←
Lead section area mm ²	1257	←	←
Rubber thickness mm	1.4	←	←
Rubber layer number mm	29	←	←
Steel plate thickness mm	1.2	←	←
Shape factor S1	33.0	36.6	←
Aspect ratio S2	5.0	4.9	←

2.2. Basic characteristics

The basic characteristics of the specimens were investigated to verify whether the characteristic values were the same for all specimens or not. Sine waves were applied in a single direction in four cycles of loading and unloading. The maximum velocity was set at 15 mm/sec. Figure 2 shows the hysteresis loops for each specimen and characteristic value in the third cycle corrected to 15°C-equivalent value. In the basic characteristics, the post-yield stiffness Kd_0 is the mean of plus and minus inclinations obtained as a result of linear regression in the amplitude range, or half the maximum amplitude. The yield load Qd_0 is the mean of plus and minus section loads based on the regression line. Investigations revealed that values were obtained in all the specimens that satisfied the design values. The hysteresis loops for S2 are shaped like *tsuzumi*, or a Japanese hand drum, because the aspect ratio of the lead plug is higher than in the other specimens. The tendency is greater in S2 than in a full-scale LRB because of the scale effect where a small specimen is used.

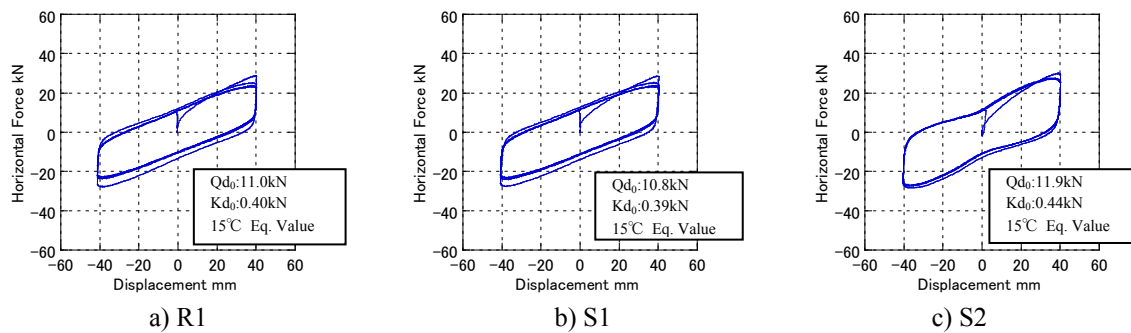


Figure 2. Basic characteristics

3. LOADING APPARATUS

A 0.5-kN triaxial testing apparatus was developed to apply bi-directional horizontal loading to LRBs (Figure 3). The main features of the apparatus are listed in Table 1. In the triaxial testing apparatus, the horizontal main axis (x axis) actuator on the bottom platen and the horizontal sub axis (y axis) on the top platen are mounted perpendicular to each other on the frame. Thus, bi-directional horizontal loading can be applied. A six degree of freedom load cell is installed between the bottom platen and movable part, which enables the detection of six elements of force on the specimen free from the influence of friction in the movable part.

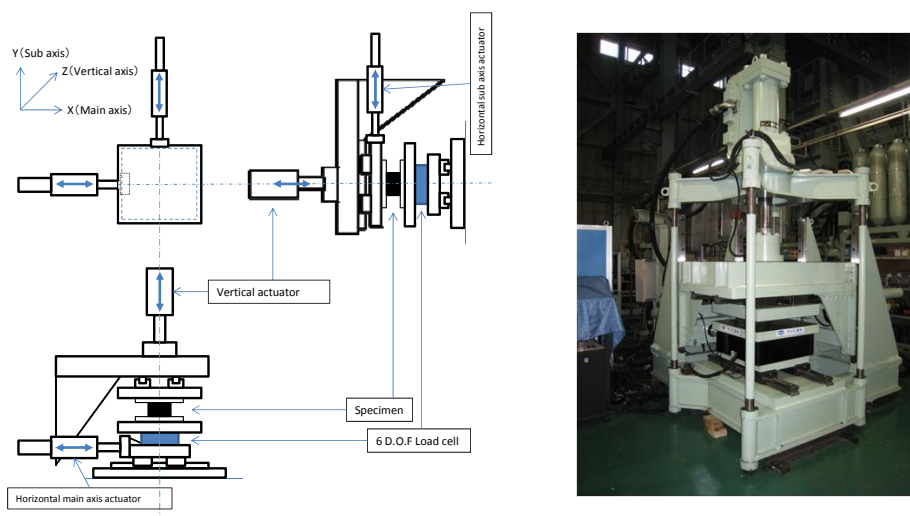


Figure 3. 0.5MN triaxial testing apparatus

Table1. Main features of testing apparatus

Vertical force (kN)	Horizontal force (kN)		Horizontal displacement (mm)		Horizontal velocity (mm/s)	
	X	Y	X	Y	X	Y
500	200	100	+/-250	+/-250	300	300

4. LOADING METHOD

First, how to give input displacement for bi-directional horizontal loading is described. The bi-directional horizontal displacement waves to be given to the specimen were developed by giving phase difference θ to a sine wave with certain amplitude A_0 as expressed in equation (1)

$$\begin{cases} D_{x0} = A_0 \sin(\phi) \\ D_{y0} = A_0 \sin(\phi + \theta) \end{cases} \quad (1)$$

where, A_0 is an amplitude parameter and θ is a phase difference parameter. Equation (1) is an expansion of a displacement under unidirectional horizontal loading to another under bi-directional horizontal loading. The value of phase difference θ can represent the orbit of displacement under unidirectional to elliptical and circular loading

Input displacement wave has origins at the start and end of the displacement orbit. The start and end were positioned at the start and end of the cycle of unidirectional to elliptical and circular loading. Displacement waves obtained by inputting phase-difference-based displacements are shown in Figure 4. The orbits of displacement are shown in Figure 5. In the test, the number of cycles of unidirectional, elliptical or circular loading was set at three. In order to match the direction of horizontal main axis actuator and the main axis direction of an elliptical orbit (x direction), the displacements to be given to the main and sub axis actuators were obtained using equation (2)

$$\begin{Bmatrix} D_x \\ D_y \end{Bmatrix} = \begin{bmatrix} \cos 45^\circ & \sin 45^\circ \\ -\sin 45^\circ & \cos 45^\circ \end{bmatrix} \begin{Bmatrix} D_{x0} \\ D_{y0} \end{Bmatrix} \quad (2)$$

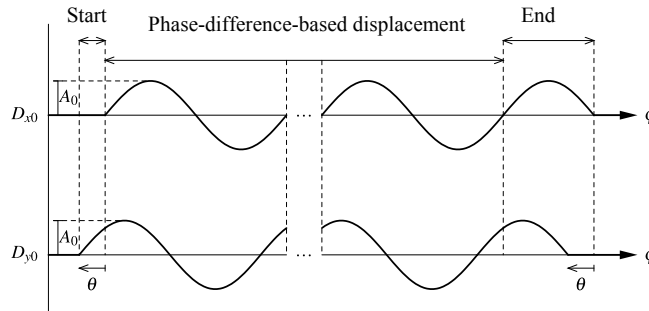


Figure4. Displacement waves

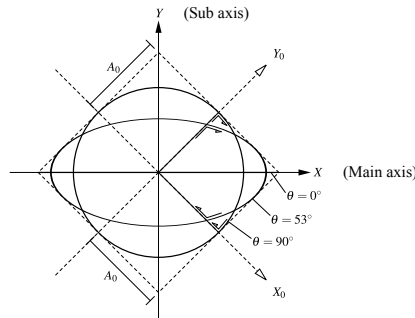


Figure5. Orbit of displacement

Shown below is a method of specifying the amplitude parameter of input wave during loading. For the displacement orbit determined by equation (1), the amplitude of the elliptical orbit in the main axis direction A_x and amplitude in the sub axis direction A_y were obtained by equation (3)

$$\begin{cases} A_x = \sqrt{2}A_0 \cos\left(\frac{\theta}{2}\right) \\ A_y = \sqrt{2}A_0 \sin\left(\frac{\theta}{2}\right) \end{cases} \quad (3)$$

For the shape of the input displacement orbit, phase difference parameter θ was determined by equation (4) based on the amplitude ratio A_y/A_x .

$$\theta = 2 \tan^{-1}(A_y/A_x) \quad (4)$$

For amplitude parameters, amplitude ratios of 0, 0.5 and 1.0 were used, which corresponded to the displacement orbit under unidirectional horizontal loading, elliptical orbit with a 2:1 ratio of long and short axes and circular orbit, respectively. Phase difference parameter θ was 0° , 53.13° and 90° .

For determining the amplitude of input displacement, the shear strain of laminated rubber at a phase difference θ of 0° (unidirectional orbit) was designated as a representative value (hereinafter referred to as strain level γ). Strain level γ was specified in increments of 50% in the 50-400% range. Amplitude parameter A_0 was determined using equation (5).

$$A_0 = \gamma H / \sqrt{2} \quad (5)$$

where, H is the total thickness of rubber layers. Table 2 shows combinations of amplitude ratio, strain level and loading pattern. Three specimens of each type were developed. Each was applied to the amplitude ratios listed in Table 2.

Table2. Loading patterns

		Shape of displacement orbit					
		Amplitude ratio: 0.0 (unidirectional)		0.5 (2:1 elliptical)		1.0 (circular)	
		Phase difference $\theta = 0.00^\circ$		$\theta = 53.13^\circ$		$\theta = 90.00^\circ$	
		Main axis amplitude	Sub axis amplitude	Main axis amplitude	Sub axis amplitude	Main axis amplitude	Sub axis amplitude
Strain level γ (%)	50	50.0	0.0	44.7	22.4	35.4	35.4
	100	100.0	0.0	89.4	44.7	70.7	70.7
	150	150.0	0.0	134.2	67.1	106.1	106.1
	200	200.0	0.0	178.9	89.4	141.4	141.4
	250	250.0	0.0	223.6	111.8	176.8	176.8
	300	300.0	0.0	268.3	134.2	212.1	212.1
	350	350.0	0.0	313.0	156.5	247.5	247.5
	400	400.0	0.0	375.8	178.9	282.8	282.8

5. Test results

5. 1. Hysteresis loops

The hysteresis loops obtained in the tests under respective loading patterns are shown in Figures 6 through 8. The hysteresis loops show from left to right the results of a) unidirectional loading, b) elliptical loading and c) circular loading. The hysteresis loops under unidirectional loading are similar for R1 and S1 with varying cross sections. Thus, no variations of loops were found according to the cross section. The area surrounded by the loops is slightly larger for S2 than for the other specimens because of the fluctuation of the production of specimens. The hysteresis loops for the main axis under

elliptical loading were similar in all specimens. In the sub axis direction, hysteresis loops were shaped like a diamond, typical of elliptical loading. The hysteresis loops under circular loading are similar in the main and sub axis directions. The loops are rounded at the maximum displacement.

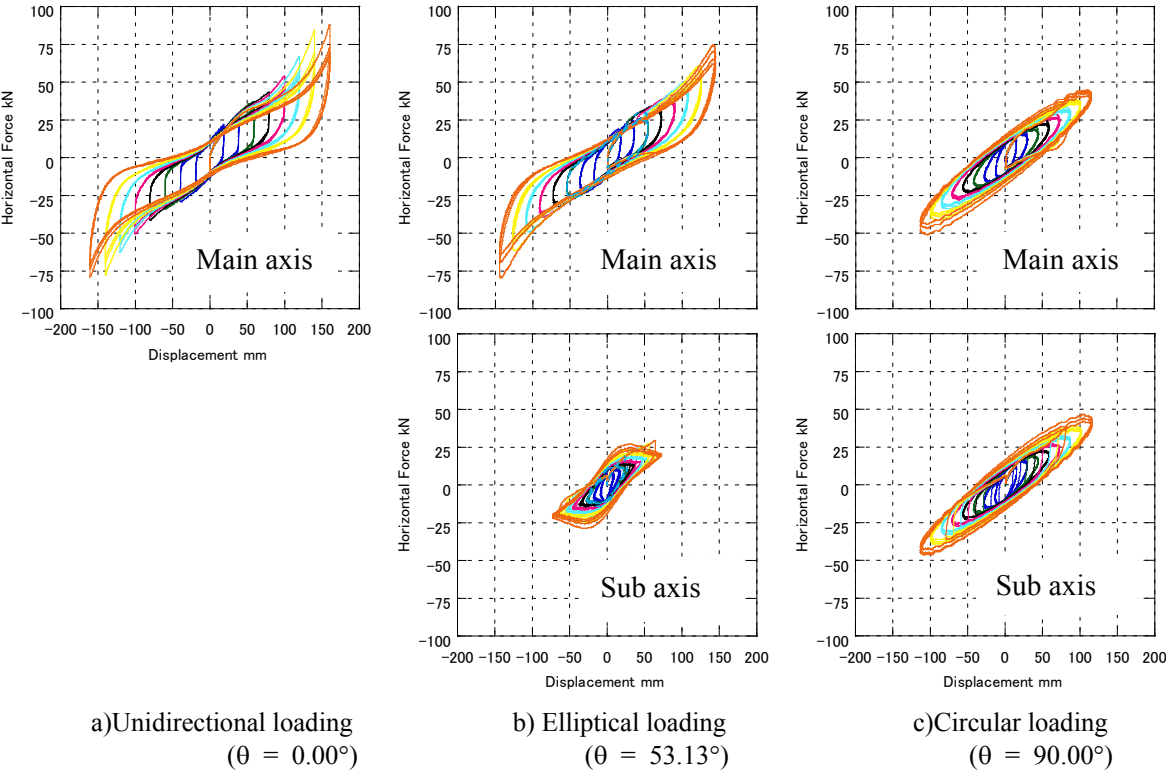


Figure6. Hysteresis loops for R1

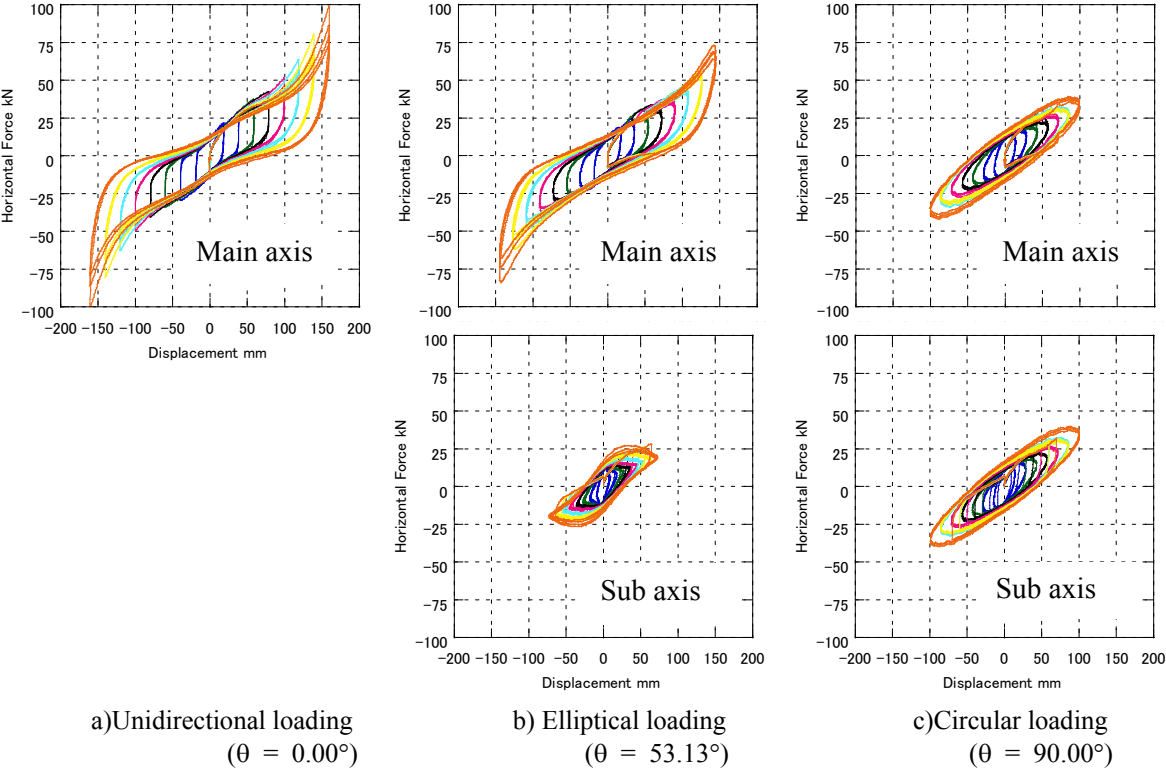


Figure7. Hysteresis loops for S1

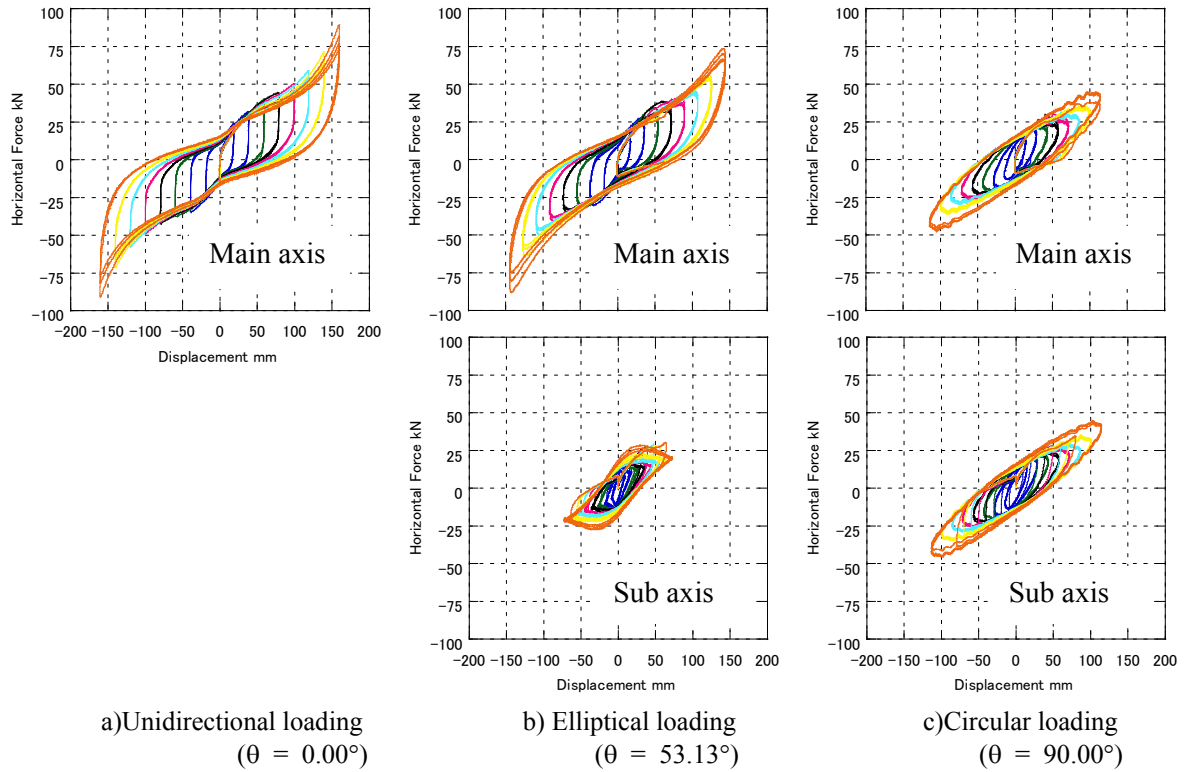


Figure8. Hysteresis loops for S2

5.2. Characteristic values

The indexes of yield load Q_d and post-yield stiffness K_d at each input strain level obtained in the tests are shown in Figure 9. Q_d is the mean of plus and minus section loads. K_d is the mean of plus and minus inclinations of Q_d relative to the maximum horizontal force. No variations of Q_d were found in R1 and S1 with varying cross sections under unidirectional, elliptical or circular loading. Q_d of S2 with four lead plugs is different from those of the other specimens. Q_d of S2 under unidirectional loading has a similar value to those of the other specimens until the shear strain reaches approximately 150% but increases considerably in the strain area beyond. In response to input strain under bi-directional loading, post-yield values result in a curve convex upward for S2, unlike curves convex downward for R1 and S1.

The variations of post-yield stiffness K_d in response to input strain exhibit curves convex downward regardless of the specimen.

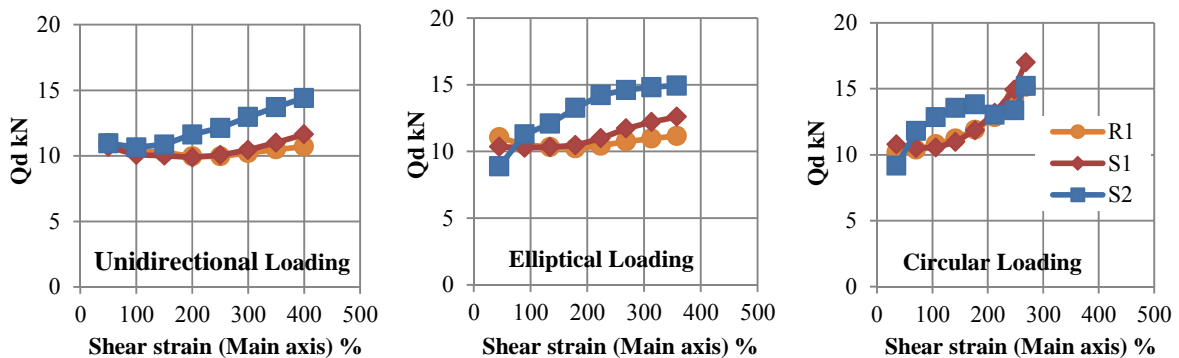


Figure9. Post-yield load Q_d

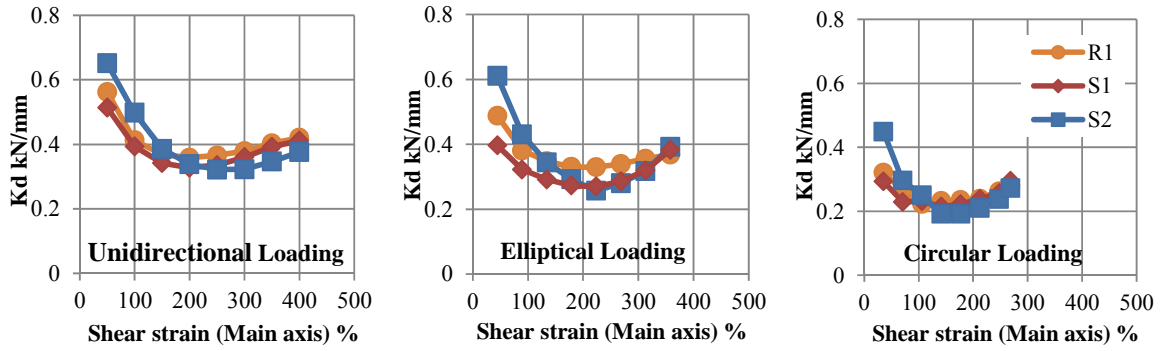


Figure10. Post-yield stiffness Kd

5.3. Torsional moment

Applying bi-directional horizontal loading to a laminated rubber bearing with damping properties like an LRB induces torsional moment along the height of the laminated rubber. The mechanism of torsional moment generation is explained as shown in Figure 11. The horizontal reaction of an LRB under bi-directional horizontal loading can be dissolved into the rubber force toward the origin of the loading orbit and the lead plug force in the tangential direction of the loading orbit. Then, there occurs a deviation between the LRB horizontal force and the origin of the loading orbit at an angle of θ . The deviation between the LRB horizontal force and the origin causes torsional moment in the LRB. The LRB horizontal force with a deviation of θ can be dissolved into the forces in the x and y directions, f_x and f_y . These horizontal forces are equally carried by the upper and lower flanges of the specimen. The torsional moment that occurs at the upper and lower flanges M_t is expressed by

$$M_t = \frac{f_y \cdot \delta_x - f_x \cdot \delta_y}{2} \quad (6)$$

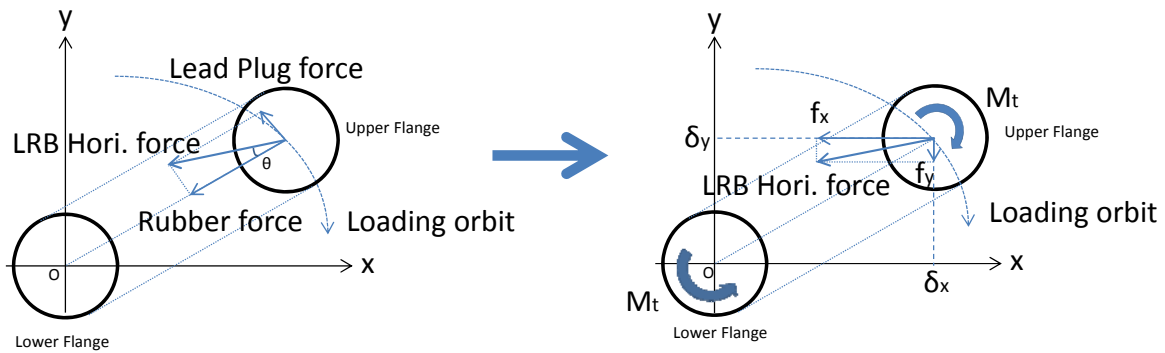


Figure11. Mechanism of torsional moment generation

In this study, the torsional moment in LRB was measured using a six degree of freedom load cell in the test apparatus, and the relationship between the maximum torsional moment and each input strain in the main axis under elliptical and circular loading was organized (Figure 12). The maximum torsional moment under bi-directional loading of LRB was the same regardless of the specimen. Torsional moment increased with the input strain, and the inclination was the same either under elliptical or circular loading.

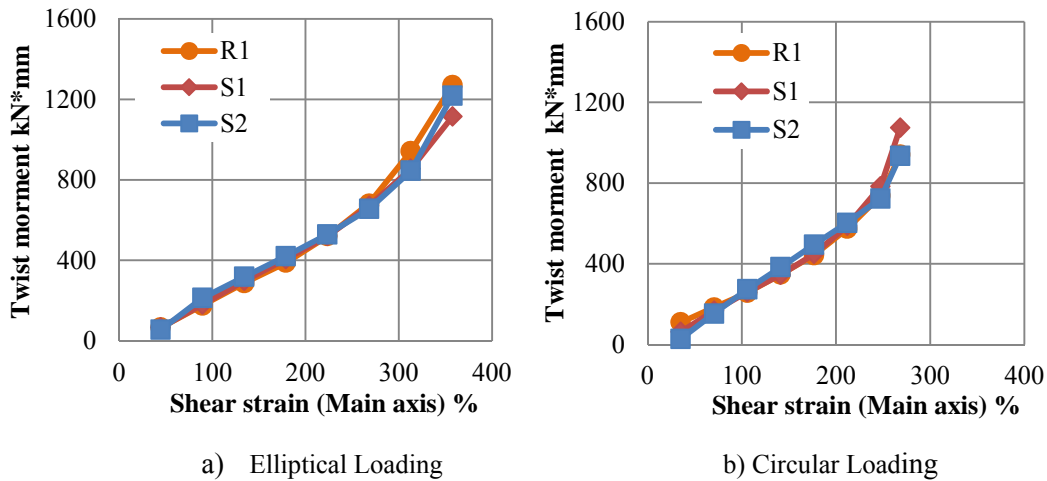


Figure12. Twist moment relativ on shar strain

5.4. Torsional deformation

The torsional deformation of each specimen was investigated using the video images obtained during loading. In order to confirm the state of torsional deformation of the specimen, part of the rubber was removed and marks were made in the vertical direction. Figure 13 shows images for analysis in the third cycle of circular loading at a strain level of 400%. Figure 13 shows the occurrence of torsional deformation in the LRB. Torsional deformation is smaller in S2 than in R1 although the deformation seems the same in both specimens.

The distributions of torsional deformations under bi-directional horizontal loading obtained in image analysis are shown in Figure 14. The torsional deformations under elliptical loading (Figure 14 a)) were the same regardless of the specimen up to an input level of 250%. The distributions of torsional deformations at an input level of 300%, however, are shown in the descending order from R1 to S1 and S2. At an input level of 350%, the distribution is larger in R1 than in S1 and distributions are nearly the same in S1 and S2. Under circular loading (Figure 14 b)), torsional deformation was the same regardless of the specimen up to an input level of 250% as under elliptical loading. The distributions of torsional deformations at input levels of 300 and 350%, however, are shown in the descending order from S1 to R1 and S2. At an input level of 400%, the distribution in R1 is nearly the same as in S1 and the distribution in S1 is larger than in S2. The torsional displacement under bi-directional horizontal loading is generally smaller in the S2 specimen with four lead plugs.

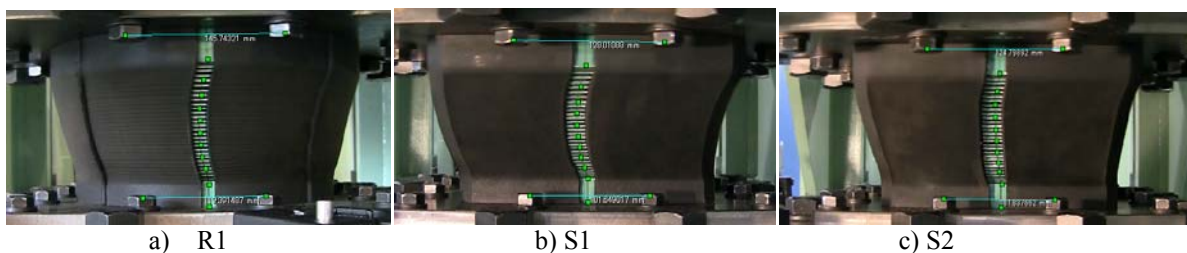


Figure13. Occurrence of torsional deformation ($\gamma=400\%$, $\theta=90.00$ at 3cycle)

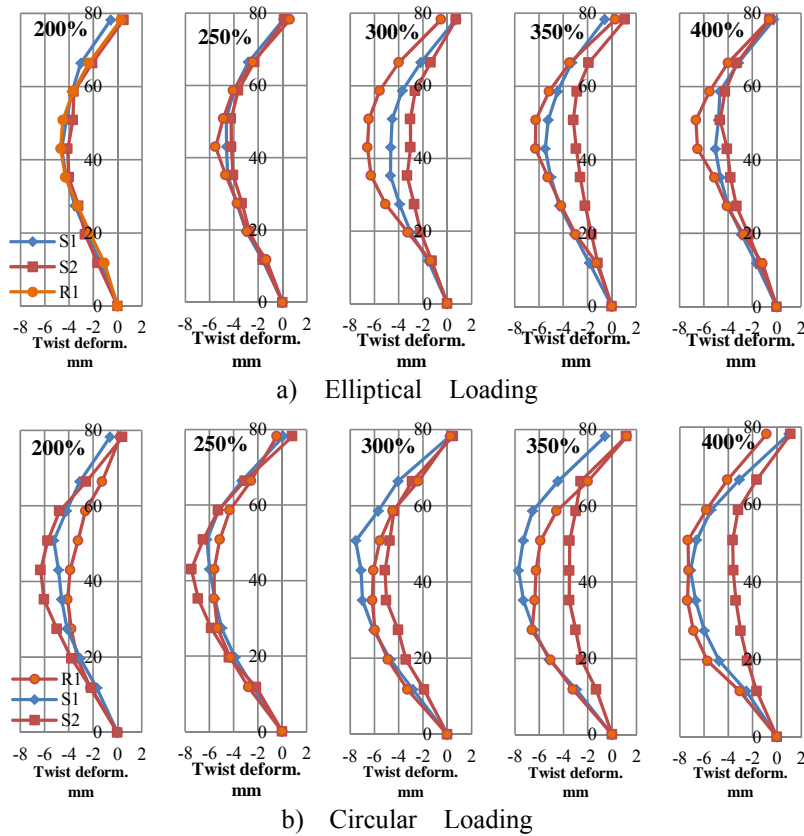


Figure14. Twist deformation

6. CONCLUSIONS

Bi-directional horizontal loading tests were conducted for three types of LRB with identical design characteristic values and varying cross sections. As a result, the following knowledge was obtained.

It was verified that the basic characteristic values of specimens R1, S1 and S2 with varying cross sections satisfied the design values and that the specimens provided similar performance. The hysteresis loops of the specimens obtained by inputting phase difference were compared with one another.

Yield load Q_d under bi-directional loading varied similarly in R1 and S1 in response to input strain. There was no difference according to the cross section. Q_d of the S2 specimen with four lead plugs, however, varied differently. The variations of post-yield stiffness K_d in response to input strain were similar regardless of the specimen. There were no variations of maximum torsional moment from specimen to specimen. The torsional deformation of LRB under bi-directional horizontal loading was small in the S2 specimen with four lead plugs.

REFERENCES

- Shortreed, J.S., Seible, F., Fikiatrault, A., and Benzoni, G, (2001) Characterization and testing of the Caltrans Seismic Response Modification Device Test System . *The Royal Society* 359, 1829-1580
- Minewaki S., Yamamoto M., Higashino M., Hamaguchi H., Kyuke H., Sone T., Yoneda H. (2009). Performance tests of full size isolators for super high-rise isolated buildings. *J. of Structural Engineering, AIJ*, 55B, 469-477 (in Japanese).
- Nakamura, T., Kouchiyama, O., Nagata, S., Ikenaga, M., Wada, A., (2011) Bi-directional test on real-scale square lead rubber bearing. 81th Kanto Dept. conference AIJ 301-304 (in Japanese)